



LAWRENCE  
LIVERMORE  
NATIONAL  
LABORATORY

# Transport in a highly asymmetric binary fluid mixture

S. Bastea

October 24, 2006

Physical Review E

## **Disclaimer**

---

This document was prepared as an account of work sponsored by an agency of the United States Government. Neither the United States Government nor the University of California nor any of their employees, makes any warranty, express or implied, or assumes any legal liability or responsibility for the accuracy, completeness, or usefulness of any information, apparatus, product, or process disclosed, or represents that its use would not infringe privately owned rights. Reference herein to any specific commercial product, process, or service by trade name, trademark, manufacturer, or otherwise, does not necessarily constitute or imply its endorsement, recommendation, or favoring by the United States Government or the University of California. The views and opinions of authors expressed herein do not necessarily state or reflect those of the United States Government or the University of California, and shall not be used for advertising or product endorsement purposes.

# Transport in a highly asymmetric binary fluid mixture

Sorin Bastea\*

*Lawrence Livermore National Laboratory,*

*P.O. BOX 808, Livermore, CA 94550*

## Abstract

We present molecular dynamics calculations of the thermal conductivity and viscosities of a model colloidal suspension with colloidal particles roughly one order of magnitude larger than the suspending liquid molecules. The results are compared with estimates based on the Enskog transport theory and effective medium theories for thermal and viscous transport. We also discuss the consequences of these results to some proposed mechanisms for thermal conduction in nanocolloidal suspensions.

PACS numbers: 66.60.+a, 66.20.+d, 82.70.Dd, 83.80.Hj

---

\*Electronic address: [sbastea@llnl.gov](mailto:sbastea@llnl.gov)

Liquid suspensions of solid particles (colloids) are widely encountered in biology, industry and many natural processes. In addition to their relevance for numerous practical applications they have emerged as a useful paradigm for the study of phase transitions, from crystal nucleation and growth to gelation [1]. Colloids have not only interesting thermodynamic properties, but remarkable rheological properties as well [2] and very complex flow behavior [3]. When the suspended particles are only one to two orders of magnitude larger than typical liquid molecules, i.e. in the nanometer domain, colloids may exhibit entirely new properties [4, 5] that are expected to have important technological consequences. A theoretically important and practically relevant class of colloids consists of suspensions of spherical colloidal particles with interactions dominated by excluded volume effects. In the following we employ molecular dynamics simulations to calculate the thermal conductivity and viscosities (shear and bulk) of fairly dilute colloidal suspensions modeled as mixtures of strongly asymmetric particles interacting through short range repulsive potentials. We discuss the results in the light of theoretical estimates based on microscopic and macroscopic pictures of the system. Despite the simplicity of the model the conclusions should provide, *inter alia*, some guidance on the expected transport properties of dilute suspensions of nano-sized particles, particularly the thermal conductivity, which has been the subject of some speculation [5–7].

The model that we study consists of two types of particles, *1 - solvent* and *2 - colloid*, with masses  $m_1 \equiv m$  and  $m_2 \equiv m_c$ . The interaction potentials between the particles are based on the inverse-12, 'soft sphere' potential, whose properties have been well studied [8, 9]

$$u(r) = \epsilon \left( \frac{\sigma}{r} \right)^{12} \quad (1)$$

and which we truncate and shift at  $r/\sigma = 2$ ; we also define  $u(r) = \infty$  for  $r < 0$ . The interactions are:

$$u_{11}(r) = u(r) \quad (2)$$

$$u_{12}(r) = u(r - R_c) \quad (3)$$

$$u_{22}(r) = u(r - 2R_c) \quad (4)$$

Similar interactions, that take into account the 'size' of the colloidal particles by introducing a 'hard core radius'  $R_c$ , have been employed before to model suspensions [10, 11]. For temperatures  $k_B T \simeq \epsilon$  the effective diameters corresponding to the above interactions should

be well approximated by  $\sigma_1 = \sigma$ ,  $\sigma_{12} = R_c + \sigma$ , and  $\sigma_2 \equiv \sigma_c = 2R_c + \sigma$ , and satisfy  $\sigma_{12} = (\sigma_1 + \sigma_2)/2$ . In the following we will therefore quote as relevant quantities the 'diameter' ratio of the colloid and solvent particles,  $\sigma_c/\sigma$ , and the 'volume fractions' of the colloidal particles,  $\phi_c = \pi n_c \sigma_c^3/6$ , and the solvent,  $\phi = \pi n \sigma^3/6$ ;  $n_c$  and  $n$  are the corresponding number densities,  $n_c = N_c/V$ ,  $n = N/V$ . All the simulations presented here were performed in the microcanonical (NVE) ensemble with the average temperature set to  $k_B T = \epsilon$ .

The systems (mixtures) that we studied are summarized in Table 1, and correspond to two 'diameter' ratios, each with two mass ratios. Since for a realistic colloidal particle the ratio of its mass to that of a fluid molecule is  $m_c/m \sim (\sigma_c/\sigma)^3$ , our perhaps most practically relevant results correspond to  $m_c/m = 1000$ . However, we also analyzed the effect of a much smaller mass ratio,  $m_c/m = 1$ . The volume fractions  $\phi_c$  of the colloidal particles have been chosen low enough so that the system is rather dilute, but high enough so that a reasonable number of colloidal particles can be simulated without the need for a prohibitively large number of solvent particles. (Nevertheless,  $N$  is rather large, of the order  $10^5$ .) The pairs  $\phi$  and  $\phi_c$  for the two different diameter ratios have been chosen to yield the same system pressure  $p_0$ , corresponding to a pure solvent at  $n_0 \sigma^3 = 0.8$  ( $\phi_0 = 0.419$ ). Incidentally, we have found that this can be accomplished with very good precision (better than 1%) by using the scaling relation:

$$\frac{p(\sigma, \sigma_c, \phi, \phi_c)}{p_0(\sigma, \phi_0)} = \frac{p_{MCSL}(\sigma, \sigma_c, \phi, \phi_c)}{p_{CS}(\sigma, \phi_0)} \quad (5)$$

where  $p$  is the system pressure,  $p_{BMCSL}$  the Boublík-Mansoori-Carnahan-Starling-Leland equation of state pressure of a hard-sphere mixture [12, 13] and  $p_{CS}$  the Carnahan-Starling equation of state pressure of the hard-sphere liquid [14]. The choice of a common pressure allows an unambiguous comparison of the thermal conductivity and viscosities of the suspension with that of the reference system (pure solvent at pressure  $p_0$ ), is implicitly assumed by theories relying on macroscopic scale arguments (see below), and should also correspond to the usual experimental situations.

The calculation of the viscosities (shear and bulk) and thermal conductivity can be done in molecular dynamics simulations using the Green-Kubo relations, which express these linear transport coefficients as time integrals of auto-correlation functions of microscopic currents [15–17]. This formalism yields unambiguous definitions for the shear and bulk viscosities,

applicable to both single fluids and mixtures:

$$\eta(t) = \frac{1}{6Vk_BT} \int_0^t \left\langle \sum_{\alpha,\beta=1;\alpha\neq\beta}^3 \sigma_{\alpha\beta}(0) \sigma_{\alpha\beta}(\tau) \right\rangle d\tau \quad (6a)$$

$$\zeta(t) = \frac{1}{9Vk_BT} \int_0^t \left\langle \sum_{\alpha,\beta=1}^3 [\sigma_{\alpha\alpha}(0) - p][\sigma_{\beta\beta}(\tau) - p] \right\rangle d\tau \quad (6b)$$

where  $\hat{\sigma}$  is the microscopic stress tensor:

$$\sigma_{\alpha\beta}(\tau) = \sum_i [m_i v_{i\alpha}(\tau) v_{i\beta}(\tau) + F_{i\alpha}(\tau) r_{i\beta}(\tau)] \quad (7)$$

( $\alpha, \beta = x, y, z$ ),  $p$  is the pressure, and the viscosities  $\eta$  and  $\zeta$  are given by the  $t \rightarrow \infty$  limits of the above relations.

The treatment of thermal transport in mixtures on the other hand is more complicated due to the coupling of energy and mass transport [17]. Since this is an important but many times confusing issue we discuss it briefly below for the present case of a binary mixture (see also the discussion in [18]). The hydrodynamic equations for a binary mixture express species conservation, as well as momentum and entropy transport:

$$\frac{\partial \rho_a}{\partial t} + \nabla \cdot (\rho_a \mathbf{v}_a) = 0 \quad (8a)$$

$$\rho \frac{\partial \mathbf{v}}{\partial t} + \rho \mathbf{v} \cdot \nabla \mathbf{v} = -\nabla \cdot \mathbf{P} \quad (8b)$$

$$\rho \frac{\partial s}{\partial t} + \rho \mathbf{v} \cdot \nabla s = -\nabla \cdot \mathbf{J}_s + \Theta \quad (8c)$$

In the above equations  $\rho_a$  and  $\mathbf{v}_a$  ( $a = 1, 2$ ) are the (position and time dependent) mass densities and flow velocities of the two species, respectively;  $\rho$  is the total mass density,  $\rho = \rho_1 + \rho_2$ ;  $\mathbf{v}$  is the center of mass (“barycentric”) velocity,  $\mathbf{v} = \rho^{-1}(\rho_1 \mathbf{v}_1 + \rho_2 \mathbf{v}_2)$ ;  $\hat{\mathbf{P}}$  is the stress tensor,  $P_{\alpha\beta} = p\delta_{\alpha\beta} - P\iota_{\alpha\beta}$ , with  $p$  hydrostatic pressure and  $\hat{\mathbf{P}}\iota$  viscous stress tensor,  $P\iota_{\alpha\beta} = [\eta(\partial v_\alpha/\partial x_\beta + \partial v_\beta/\partial x_\alpha) + (\zeta - 2\eta/3)\nabla \cdot \mathbf{v}\delta_{\alpha\beta}]$ ;  $s$  is the entropy density,  $\mathbf{J}_s$  the entropy current and  $\Theta$  the entropy production. The entropy current  $\mathbf{J}_s$  is expressed in terms of heat -  $\mathbf{J}_q$ , and mass diffusion -  $\mathbf{J}_a$ , currents:

$$\mathbf{J}_s = \frac{1}{T} [\mathbf{J}_q - (\mu_1 \mathbf{J}_1 + \mu_2 \mathbf{J}_2)] \quad (9a)$$

$$\mathbf{J}_q = \mathbf{J}_e - (\rho e \mathbf{v} + \mathbf{P} \cdot \mathbf{v}) \quad (9b)$$

$$\mathbf{J}_a = \rho_a (\mathbf{v}_a - \mathbf{v}) \quad (9c)$$

, with  $\mu_a$  chemical potential (per unit mass),  $e$  total specific energy and  $\mathbf{J}_e$  the corresponding energy current. In the framework of non-equilibrium thermodynamics [17] the heat and mass currents (denoted as the set  $\{\mathbf{J}_\delta\}$ ) are connected to thermodynamic forces  $\{\mathbf{X}_\delta\}$  by heat-mass linear transport coefficients  $\{L_{\delta\gamma}\}$ , ( $\delta, \gamma = 1, 2, q$ ):

$$\mathbf{J}_\delta = \sum_{\gamma} L_{\delta\gamma} \mathbf{X}_\gamma \quad (10)$$

The entropy production  $\Theta$  contains independent contributions from 'vectorial' phenomena (heat and mass transport) -  $\Theta_v$  and 'tensorial' ones (momentum transport) -  $\Theta_t$ ,  $\Theta = \Theta_v + \Theta_t$ . Both contributions assume the Onsager form, i.e. for heat-mass processes:

$$\Theta_v = \frac{1}{T} \sum_{\delta} \mathbf{J}_\delta \cdot \mathbf{X}_\delta \quad (11)$$

while  $\Theta_t = (1/T) \hat{\mathbf{P}}' : \nabla \mathbf{v}$ . The Onsager reciprocity relations,  $L_{\delta\gamma} = L_{\gamma\delta}$ , along with  $\mathbf{J}_1 + \mathbf{J}_2 = 0$  from the definition of the diffusion currents leave 3 independent heat-mass transport coefficients for a binary mixture,  $\{L_{12}, L_{1q}, L_{qq}\}$ , with the currents now written as

$$\mathbf{J}_1 = -L_{12}(\mathbf{X}_1 - \mathbf{X}_2) + L_{1q}\mathbf{X}_q \quad (12a)$$

$$\mathbf{J}_q = L_{1q}(\mathbf{X}_1 - \mathbf{X}_2) + L_{qq}\mathbf{X}_q \quad (12b)$$

Three distinct sets of currents and thermodynamic forces have been discussed in detail [17, 18], each with different transport coefficients. The currents (and forces) of different sets are connected by linear transformations under which  $\Theta_v$  is invariant and preserves its Onsager form. This leads to well defined and useful relations between the coefficients [18]. We would like to point out that one such relation can be deduced without considering in detail the particular definitions of currents and forces. We simply note that all sets use the same, physically intuitive, heat driving force,  $\mathbf{X}_q = -\nabla T/T$ , as well as diffusion currents  $\mathbf{J}_a$  given by Eq. 9c. Since the phenomenological definition of the thermal conductivity  $\lambda$  is based on the observation that in the absence of diffusion, i.e.  $\mathbf{J}_1 = 0$ , the heat current should reduce to its canonical form,  $\mathbf{J}_q = -\lambda \nabla T$  [19], this yields

$$\lambda = \frac{1}{T} \left( L_{qq} + \frac{L_{1q}^2}{L_{12}} \right) \quad (13)$$

It is worth noting that, as opposed to  $L_{1q}$  and  $L_{qq}$ ,  $\lambda$  does not depend on the chosen set of currents and forces and moreover, it assumes the above form for all the sets.

For our calculations we adopt the 'mainstream' choice for forces (and currents),

$$\mathbf{X}_a = -T\nabla(\mu_a/T) \quad (14a)$$

$$\mathbf{X}_q = -\frac{1}{T}\nabla T \quad (14b)$$

( $a = 1, 2$ ) [18], but this selection is not in fact arbitrary. As first discussed by Erpenbeck [18], the 'mainstream' set is preferable for molecular dynamics calculations since its corresponding microscopic currents only depend on microscopic quantities easily available in simulations. The other choices on the other hand require the knowledge of thermodynamic quantities such as chemical potentials or partial enthalpies which are difficult to calculate with any accuracy (see also below).

The microscopic currents for the 'mainstream' set are

$$\mathbf{j}_a(\tau) = \sum_{i(a)} m_i [\mathbf{v}_i(\tau) - v_{CM}(\tau)] \quad (15)$$

$$\begin{aligned} \mathbf{j}_q(\tau) = & \sum_i \mathbf{v}_i(\tau) \left\{ \frac{1}{2} m_i v_i^2(\tau) + \frac{1}{2} \sum_{j \neq i} V_{ij} [r_{ij}(\tau)] \right\} \\ & + \frac{1}{2} \sum_i \sum_{j \neq i} [\mathbf{r}_i(\tau) - \mathbf{r}_j(\tau)] \mathbf{v}_i(\tau) \cdot \mathbf{F}_{ij}(\tau) - H \mathbf{v}_{CM}(\tau) \end{aligned} \quad (16)$$

where  $H$  and  $\mathbf{v}_{CM}$  are the enthalpy and center of mass velocity of the system, respectively. Since  $\mathbf{v}_{CM}$  is set to zero in the simulations,  $H$  does not enter in fact the calculations. The Green-Kubo relations for the heat-mass coefficients are:

$$L_{qq}(t) = \frac{1}{3Vk_B T} \int_0^t \langle \mathbf{j}_q(0) \cdot \mathbf{j}_q(\tau) \rangle d\tau \quad (17a)$$

$$L_{1q}(t) = \frac{1}{3Vk_B T} \int_0^t \langle \mathbf{j}_1(0) \cdot \mathbf{j}_q(\tau) \rangle d\tau \quad (17b)$$

$$L_{12}(t) = \frac{1}{3Vk_B T} \int_0^t \langle \mathbf{j}_1(0) \cdot \mathbf{j}_2(\tau) \rangle d\tau \quad (17c)$$

and  $\{L_{12}, L_{1q}, L_{qq}\}$  correspond to the  $t \rightarrow \infty$  limits of the above relations.

It has been sometimes remarked [20] that the 'mainstream' set does not allow a proper calculation of the thermal conductivity since  $\lambda$  as defined by Eq. 13 may result from the subtraction of two large quantities leading to significant errors. To avoid this perceived problem a different set of currents has been used, with microscopic heat current

$$\mathbf{j}_q'' = \mathbf{j}_q - (h_1 \mathbf{j}_1 + h_2 \mathbf{j}_2) \quad (18)$$



where  $h_{1,2}$  are the partial specific enthalpies. This is expected to shift most of the thermal conductivity contributions to the first term of Eq. 13, and therefore result in a more appropriate definition. We would like to remark that, if we define a time-dependent thermal conductivity

$$\lambda(t) = \frac{1}{T} \left[ L_{qq(t)} + \frac{L_{1q}(t)L_{q1}(t)}{L_{12}(t)} \right] \quad (19)$$

which satisfies  $\lambda = \lim_{t \rightarrow \infty} \lambda(t)$ , it is easy to show that  $\lambda(t)$ , similarly with  $\lambda$ , is also invariant under such a change of currents. Consequently, to the extent that the thermal conductivity is defined as usual from the long-time 'plateau' of  $\lambda(t)$ , using the new current Eq. 18 does not offer any real advantage.

The molecular dynamics calculation of the transport coefficients relies on Eqs. 6 and 17, whose integrands are easily calculated during simulations. We have performed such calculations for the systems described in Table 1 and also the reference (pure solvent) system. The units for viscosity and thermal conductivity have been chosen  $(mk_B T)^{1/2}/\sigma^2$  and  $(k_B^3 T/m)^{1/2}/\sigma^2$ , respectively; the time unit is  $t_0 = \sigma(m/k_B T)^{1/2}$ . In these units we find that the reference system has viscosities  $\eta_0 = 1.11$ ,  $\zeta_0 = 0.21$  and thermal conductivity  $\lambda_0 = 4.87$ . To provide an intuitive connection to the often studied hard sphere system we also estimate for the reference system a mean free time between 'collisions' of  $\tau \simeq 0.035$ .

The autocorrelation functions (integrands) corresponding to the shear viscosity - Eq. 6a, bulk viscosity - Eq. 6b, and thermal conductivity - Eqs. 14a-c, are shown in Figs. 1-5 (normalized by their  $t = 0$  values) for the reference system (where applicable) and the colloidal system with the largest size ratio,  $\sigma_c/\sigma = 15$ . One interesting feature of the shear and bulk viscosity integrands is that they are largely independent of the mass ratio  $m_c/m$ , even when it varies by three orders of magnitude. This feature also extends to the transport coefficients themselves; as shown in Fig. 6 the shear viscosity of the colloidal system with  $m_c/m = 1000$  appears to be largely similar with that of the  $m_c/m = 1$  system. Despite the fairly small colloidal 'volume fraction' the time-dependent shear viscosity  $\eta(t)$  exhibits for both  $\sigma_c/\sigma = 15$  systems a pronounced early times peak, corresponding to a significant viscoelastic response [14]. This effect appears much reduced when the diameter ratio is only slightly smaller,  $\sigma_c/\sigma = 10$  - Fig. 6. The same behavior is also observed for the bulk viscosity - Fig. 7.

The heat-mass autocorrelations - Figs. 3-5, behave qualitatively very different from the

viscosity ones as a function of the mass of the colloidal particles. We note for example that they exhibit strong oscillations for light colloidal particles, i.e. for  $m_c = m$ , and a much smoother character for heavy ones, i.e. for  $m_c/m = 1000$ . The thermal conductivity  $\lambda(t)$  itself reflects these differences both at early times and as  $t \rightarrow \infty$ .

In the following we would like to compare the MD results for  $\eta$ ,  $\zeta$  and  $\lambda$  with available theories for transport in suspensions. The prediction of the transport properties of the present model colloidal suspension can proceed in principle along two different paths. The first path views the suspending liquid as a structureless matrix (continuum) and the colloidal particles as 'impurities' (or 'dispersed phase') with well defined properties distinct from those of the matrix. Then, by evaluating the response of the system to small, macroscopically applied fields, e.g. large scale temperature gradients or imposed shear flows, the equivalent, effective transport properties of the system can be determined (see, for example, Refs. [21, 22]). This method has a long history and is commonly known as effective medium theory (EMT). It has been successfully applied to both liquids and solids containing 'impurities' which are large compared to any inherent matrix structure and sufficiently far away from each other, i.e. dilute. The predictions of these theories typically depend only on the volume fraction  $\phi$  occupied by the dispersed phase [23], as well as 'matrix' and 'dispersed phase' properties. For dilute enough systems the  $\phi$  dependence is with a good approximation linear. When applied to the present case, where the colloidal particles considered are both 'solid' and thermally 'insulating', the transport coefficients will therefore be functions of the liquid 'matrix' properties alone, arguably at the same pressure and temperature. Such relations have been in use for more than a century, and yield for the suspension viscosity [19, 21, 24],

$$\eta_{eff} = \eta_0(1 + \frac{5}{2}\phi) \quad (20)$$

(Einstein's result for the viscosity of a dilute suspension), while for the thermal conductivity [22]

$$\lambda_{eff} = \lambda_0(1 - \frac{3}{2}\phi) \quad (21)$$

For the bulk viscosity the only similar result that appears to be available [25] suggests that there is no contribution to the effective bulk viscosity to first order in  $\phi$ . Considering the above relations, the application of EMT to the present system would therefore seem to be straightforward and require only the value of the volume fraction  $\phi$  occupied by the impurities, i.e. colloidal particles. Unfortunately this value is rather ambiguous when the

modeling is done at the microscopic level, particularly when the size of the impurities is comparable with the size of the fluid particles, as is the case here. The problem is that EMT interprets  $1 - \phi$  as the volume fraction occupied by the fluid matrix, which is itself equivocal and can be defined as either  $1 - \phi_c$ , or perhaps better for small enough volume fractions  $\phi_c$ , as  $1 - \phi'_c$ , where  $\phi'_c = \phi_c(1 + \sigma/\sigma_c)^3$  [10]. Although the difference between  $\phi_c$  and  $\phi'_c$  is not completely negligible, and we quote effective medium theory predictions corresponding to both of them, this does not affect our conclusions.

The second, conceptually different treatment of transport in suspensions regards the system as a binary fluid mixture, i.e. it considers its microscopic, particle character and its detailed interparticle interactions. While no fully microscopic theory for the transport coefficients of either simple fluids or mixtures is available, the Enskog theory (ET) for the hard sphere fluid has proved to be successful in a significant thermodynamic domain [26], and with suitable modifications has been shown to be applicable to other relevant simple fluids [27, 28]. The corresponding theory for hard sphere mixtures has also been rigorously derived [29], and tested using MD simulations for a number of relevant cases [18, 30, 31]. Although the binary mixture studied here is modeled by 'soft sphere'-based potentials and not hard spheres, we employ a simple scaling relation to estimate the relative values of the mixture transport coefficients with respect to those of the reference system at the same pressure and temperature, i.e.

$$\Xi(\sigma, \sigma_c, \phi, \phi_c, m, m_c)/\Xi_0(\sigma, \phi_0, m) = \Xi_{ET}(\sigma, \sigma_c, \phi, \phi_c, m, m_c)/\Xi_{ET0}(\sigma, \phi_0, m), \quad (22)$$

where  $\Xi$  stands for  $\eta$ ,  $\zeta$  or  $\lambda$ , and 0 denotes the reference (pure solvent) system. The Enskog theory hard sphere results (denoted above by  $ET_0$ ) are well known [26], while the Enskog mixture theory relations can be found in [29]; they are too complicated to be meaningfully quoted here. We used the second Enskog approximation [29] and tested our numerical implementation against the values quoted in [31].

We now proceed to compare the MD simulation results for shear and bulk viscosities and thermal conductivity with the predictions of these two theories - see Table 2. (We note first that the quoted MD values carry statistical error bars of approximately 10-15%, which should also encompass small deviations due to the neglect of long time tails [30, 31].) The MD calculated shear viscosity is fairly well reproduced by the effective medium theory Eq. 20 for both large and small colloidal masses. The Enskog predictions on the other

hand appear to deviate significantly from the MD values, particularly for the larger colloidal particles. Surprisingly, the opposite seems to hold for the bulk viscosity, which is found to be much larger than that of the reference system, in good agreement with the Enskog results but not EMT. The apparent failure of EMT for the bulk viscosity may signal that the theory needs significant corrections for 'soft' colloidal particles, or perhaps even for standard hard cores. The comparison of the MD values and theoretical predictions for the thermal conductivity yields the more interesting results. For heavy colloidal particles both the EMT and Enskog predictions appear to be in reasonable agreement with the MD simulations. On the other hand, if the colloidal particles are light,  $m_c/m = 1$ , particularly if the size ratio is also large, the thermal conductivity is found to be significantly bigger than the EMT prediction. In fact, for  $\sigma_c/\sigma = 15$  it appears that by adding to the solvent (at constant pressure) thermally insulating but rather small and light colloidal particles, the thermal conductivity is significantly ( $\simeq 50\%$ ) enhanced over that of the reference, pure solvent! The Enskog theory predictions also appear to roughly reproduce this trend.

In conclusion, we performed MD calculations of the viscosities and thermal conductivity of a model colloidal suspension with colloidal particles approximately only one order of magnitude larger than the solvent molecules ("nanocolloidal" suspension). The results suggest that, quite remarkably, the standard effective medium theory (EMT) remains well applicable for predicting both the shear viscosity and thermal conductivity of such suspensions when the colloidal particles have a 'typical' mass, i.e.  $m_c/m \sim (\sigma_c/\sigma)^3$ . For the bulk viscosity the available EMT result fails to reproduce the calculated values, which may indicate that some revised theory is necessary. Estimates of the transport coefficients based on the Enskog transport theory are less conclusive, but appear to suggest that when applied to systems as the ones studied here, the theory is rather inaccurate for the shear viscosity, although it may remain satisfactory for the bulk viscosity and the thermal conductivity. For extremely light colloidal particles, i.e.  $m_c/m \sim 1$ , we find a significant thermal conductivity enhancement over the EMT predictions, which is roughly reproduced by the Enskog mixture theory. This effect may be perhaps attributed to the solvent "stirring" action of the Brownian colloidal particles' motion, posited for example in [32]. However interesting, this behavior does not appear to be of much relevance for typical, realistic suspensions, including nanocolloidal ones or so-called nanofluids.

This work was performed under the auspices of the U. S. Department of Energy by

- [1] V.J. Anderson, H.N.W. Lekkerkerker, *Nature* **416**, 811 (2002).
- [2] I.M. de Schepper, H.E. Smorenburg, E.G.D. Cohen, *Phys. Rev. Lett.* **70**, 2178 (1993).
- [3] M.D. Haw, *Phys. Rev. Lett.* **92**, 185506 (2004).
- [4] D.T. Wasan, A.D. Nikolov, *Nature* **423**, 156 (2003).
- [5] P. Keblinski, S.R. Philpot, S.U.S. Choi, J.A. Eastman, *Int. J. Heat Mass Transfer* **45**, 855 (2002) and references therein.
- [6] D.H. Kumar, H. Patel, V.R.R. Kumar, T. Sundarajan, T. Pradeep, S.K. Das, *Phys. Rev. Lett.* **93**, 144301 (2004).
- [7] S. Bastea, *Phys. Rev. Lett.* **95**, 019401 (2005).
- [8] W.G. Hoover, M. Ross, K.W. Johnson, D. Henderson, J.A. Barker, B.C. Brown, *J. Chem. Phys.* **52**, 4931 (1970).
- [9] W.T. Ashurst, W.G. Hoover, *Phys. Rev. A* **11**, 658 (1975).
- [10] M.J. Nuevo, J.J. Morales, D.M. Heyes, *Phys. Rev. E* **58**, 5845 (1998).
- [11] S. Bastea, *Phys. Rev. Lett.* **96**, 028305 (2006).
- [12] T. Boublík, *J. Chem. Phys.* **53**, 471 (1970).
- [13] G.A. Mansoori, N.F. Carnahan, K.F. Starling, T.W. Leland, *J. Chem. Phys.* **54**, 1523 (1971).
- [14] J.-P. Hansen, I.R. McDonald, *Theory of Simple Liquids*, 2<sup>nd</sup> edition, (Academic Press, London, 1986).
- [15] H.S. Green, *J. Math. Phys.* **2**, 344 (1961).
- [16] R. Zwanzig, *J. Chem. Phys.* **43**, 714 (1965).
- [17] S.R. de Groot, P. Mazur, *Nonequilibrium Thermodynamics*, (Dover Publications, Inc., New York, 1984).
- [18] J.J. Erpenbeck, *Phys. Rev. A* **39**, 4718 (1989).
- [19] L.D. Landau, E.M. Lifshitz, *Fluid mechanics*, 2<sup>nd</sup> edition, (Butterworth-Heinemann, Oxford, 2000).
- [20] See, e.g., B. Bernu, J.P. Hansen, *Phys. Rev. Lett.* **48**, 1375 (1982).
- [21] G.K. Batchelor, *An Introduction to Fluid Mechanics*, Chapter 4, (Cambridge University Press,

- Cambridge, 1967).
- [22] S. Torquato, *Random Heterogeneous Materials*, Chapter 19 (Springer-Verlag, New York, 2002).
  - [23] See however S. Torquato, M.D. Rintoul, Phys. Rev. Lett. **75**, 4067, (1995) for a treatment taking into account the properties of the 'matrix'-'impurity' interface.
  - [24] See also G.K. Batchelor, J. Fluid Mech. **83**, 97 (1977) for the  $O(\phi^2)$  corrections to this result and R. Verberg, I.M. de Schepper, E.G.D. Cohen, Phys. Rev. E. **55**, 3143 (1997) for a more general treatment.
  - [25] H. Jorquera, J.S. Dahler, J. Chem. Phys. **101**, 1392 (1994).
  - [26] B.J. Alder, D.M. Gass, T.E. Wainwright, J. Chem. Phys. **53**, 3813 (1970).
  - [27] H.J.M. Hanley, R.D. McCarty, E.G.D. Cohen, Physica **60**, 322 (1972).
  - [28] S. Bastea, Phys. Rev. E **68**, 031204 (2003).
  - [29] M.L. de Haro, E.G.D. Cohen, J.M. Kincaid, J. Chem. Phys. **78**, 2746, (1983).
  - [30] J.J. Erpenbeck, Phys. Rev. A **45**, 2298 (1992).
  - [31] J.J. Erpenbeck, Phys. Rev. E **48**, 223 (1993).
  - [32] R. Prasher, P. Bhattacharya, P.E. Phelan, Phys. Rev. Lett. **94**, 025901 (2005).

TABLE I: Colloidal systems studied.

$\sigma_c/\sigma$	$m_c/m$	$N_c$	$\phi$	$\phi_c$
10	1	25	0.384	0.0751
10	1000	25	0.384	0.0751
15	1	20	0.382	0.0824
15	1000	20	0.382	0.0824

TABLE II: Comparison of the shear and bulk viscosities, and thermal conductivity (top to bottom) of the colloidal suspensions from MD simulations, effective medium theory (EMT) and Enskog theory for mixtures. The two EMT numbers correspond to volume fractions  $\phi_c$  and  $\phi'_c$  (see text).

$\sigma_c/\sigma$	$m_c/m$	<i>MD</i>	<i>EMT</i>	<i>Enskog</i>
10	1	1.12	1.19-1.25	1.34
10	1000	1.16	1.19-1.25	1.59
15	1	1.15	1.21-1.25	1.54
15	1000	1.21	1.21-1.25	1.86
10	1	1.78	1	1.44
10	1000	1.95	1	1.83
15	1	1.86	1	1.71
15	1000	2.20	1	2.22
10	1	0.95	0.85-0.89	1.26
10	1000	0.85	0.85-0.89	0.91
15	1	1.52	0.85-0.88	1.40
15	1000	0.80	0.85-0.88	0.91

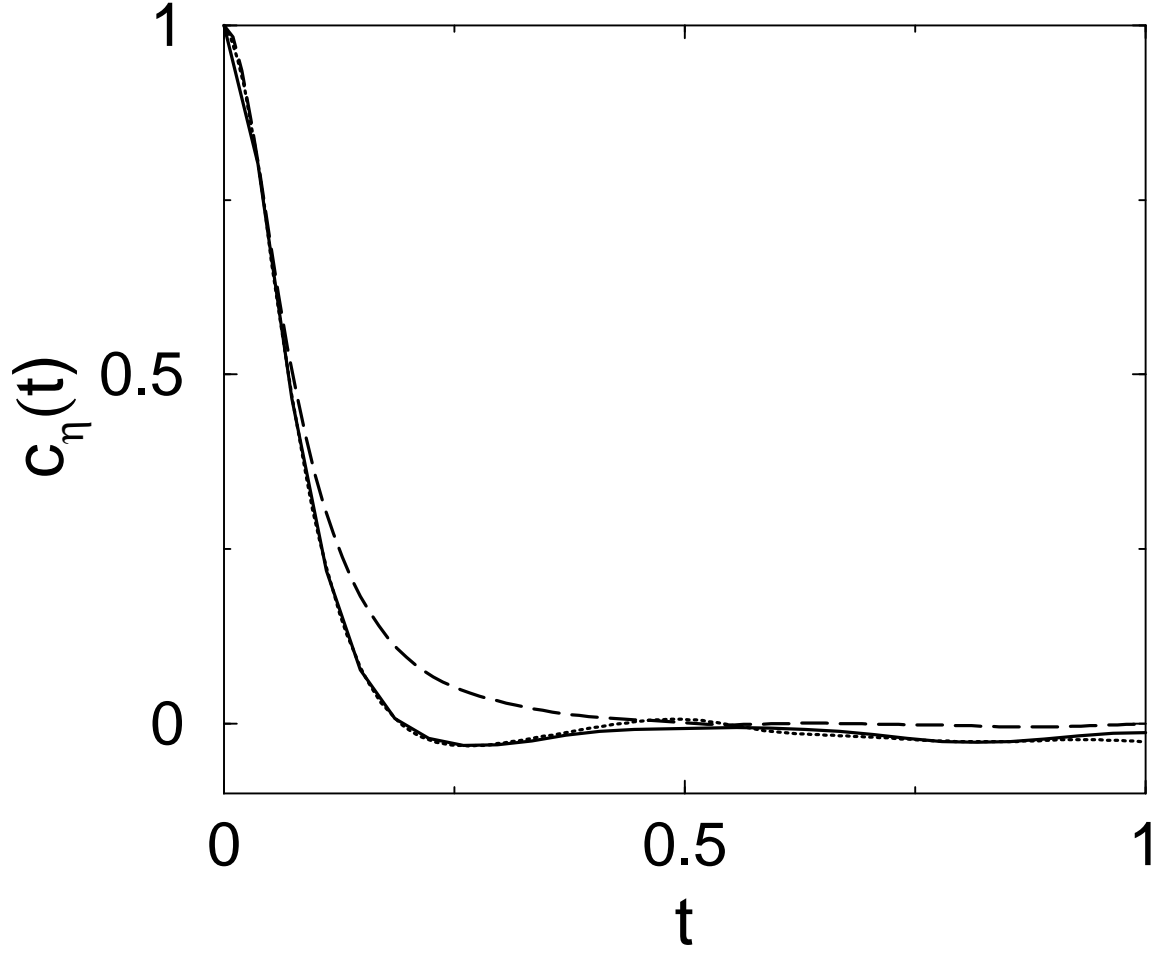


FIG. 1: Shear viscosity autocorrelation function (see text) for the reference system (dashed line), and mixtures with  $\sigma_c/\sigma = 15$ ;  $m_c/m = 1000$  (solid line) and  $m_c/m = 1$  (dotted line).



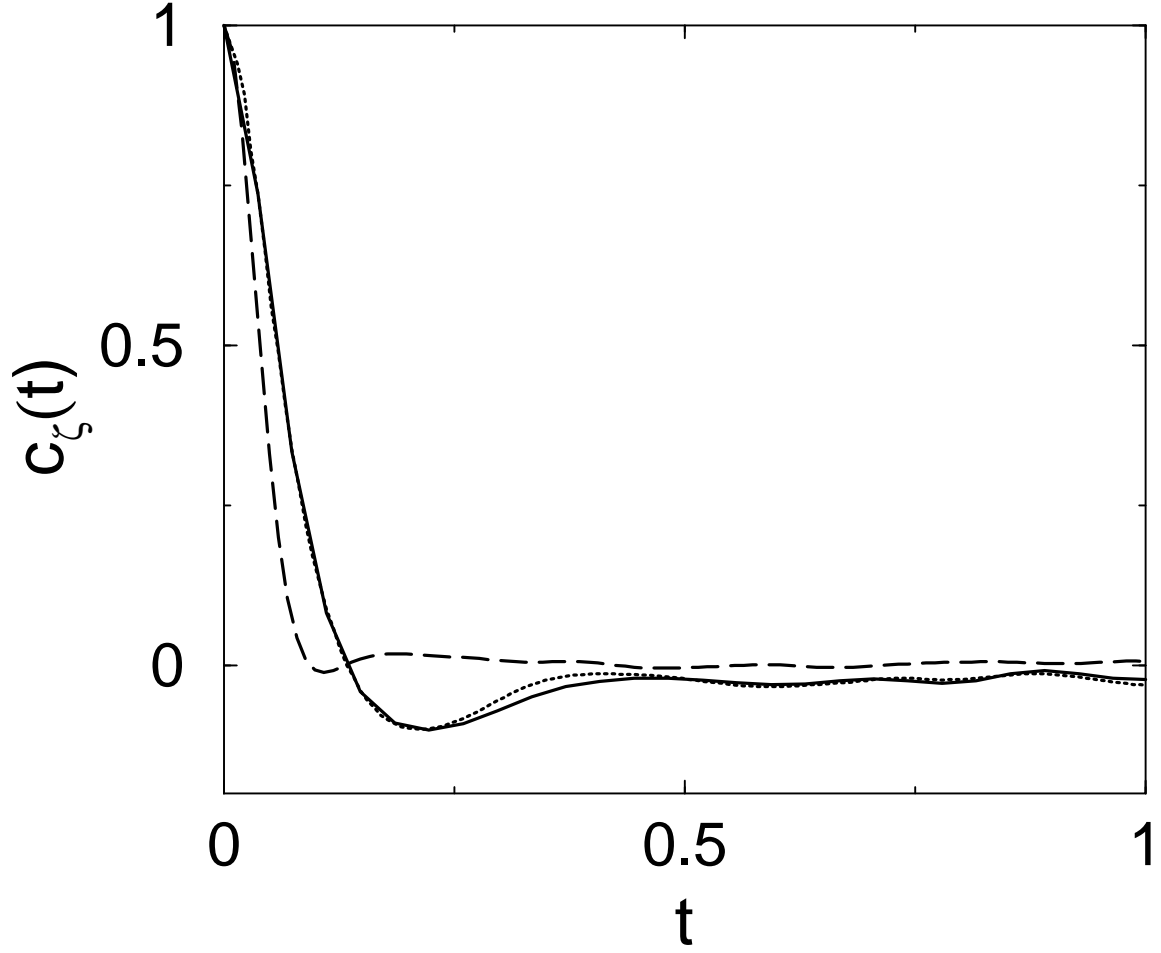


FIG. 2: Bulk viscosity autocorrelation function (see text) for the reference system (dashed line), and mixtures with  $\sigma_c/\sigma = 15$ ;  $m_c/m = 1000$  (solid line) and  $m_c/m = 1$  (dotted line).

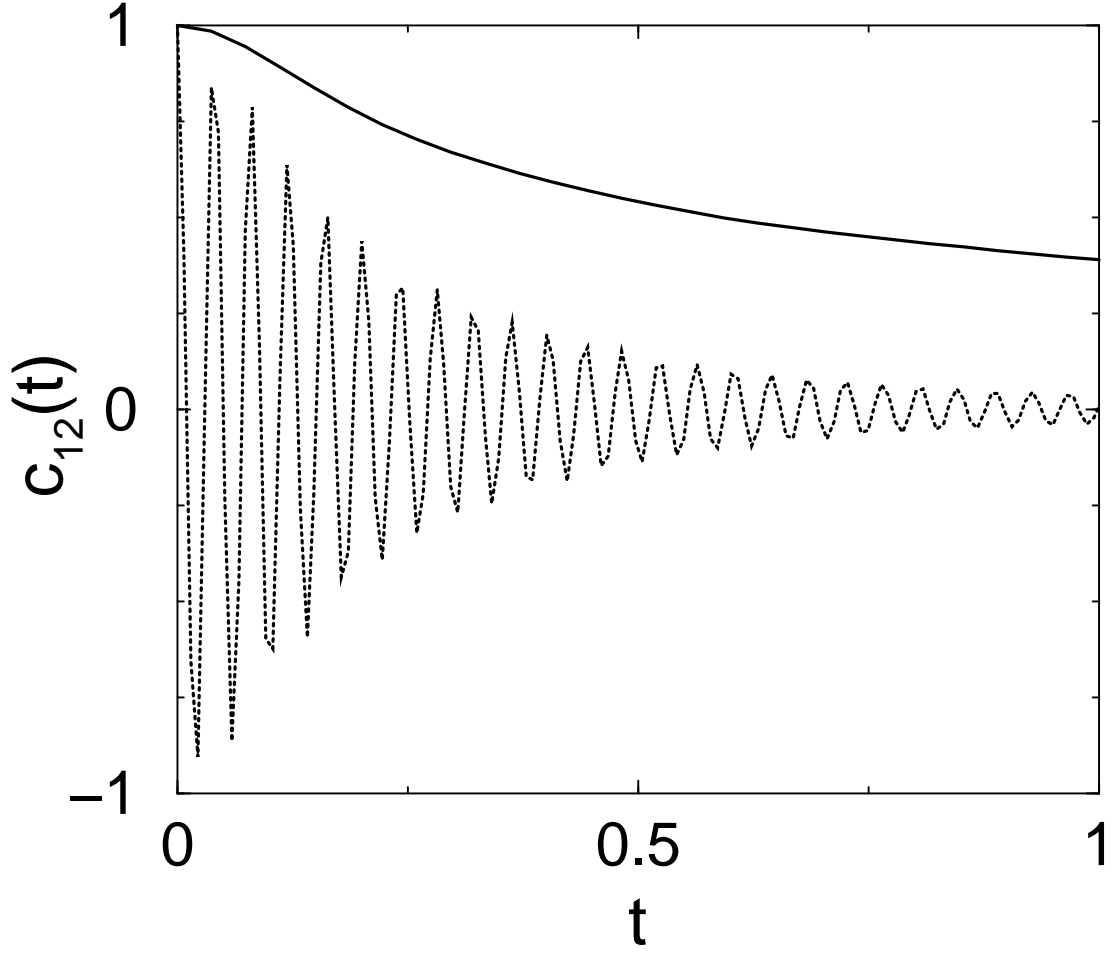


FIG. 3: Autocorrelation function for the  $L_{12}$  coefficient of mixtures with  $\sigma_c/\sigma = 15$ ;  $m_c/m = 1000$  (solid line), and  $m_c/m = 1$  (dotted line).

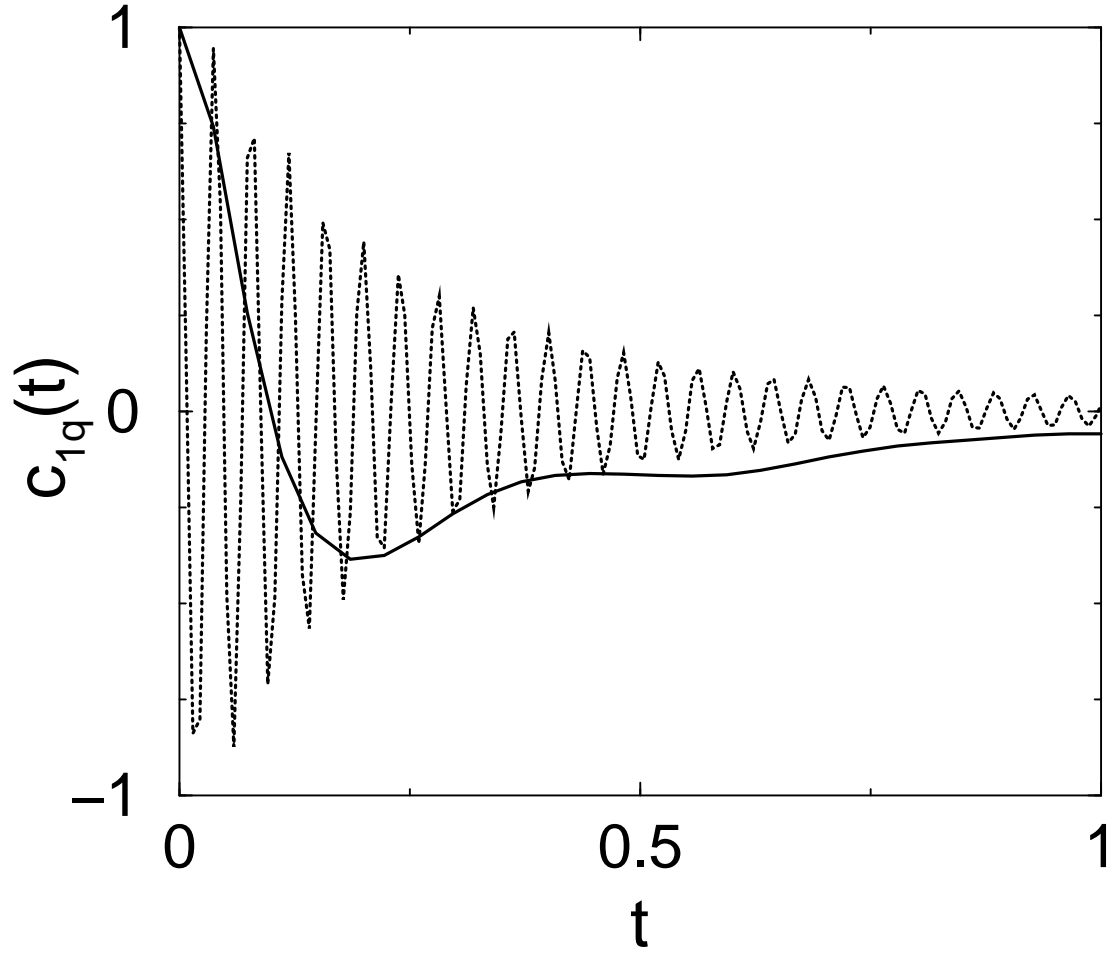


FIG. 4: Autocorrelation function for the  $L_{1q}$  coefficient of mixtures with  $\sigma_c/\sigma = 15$ ;  $m_c/m = 1000$  (solid line), and  $m_c/m = 1$  (dotted line).

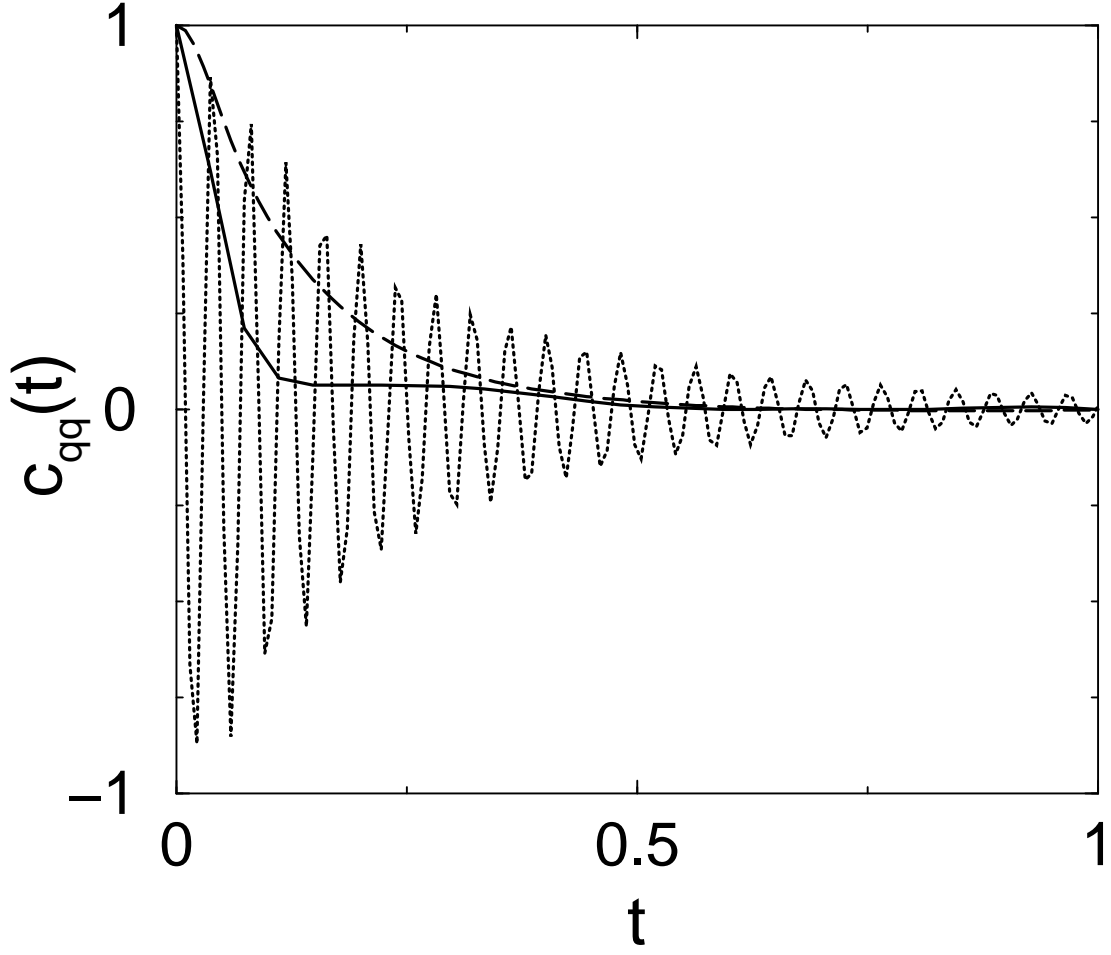


FIG. 5: Autocorrelation function for the  $L_{qq}$  coefficient of the reference system (dashed line), and mixtures with  $\sigma_c/\sigma = 15$ ;  $m_c/m = 1000$  (solid line) and  $m_c/m = 1$  (dotted line).

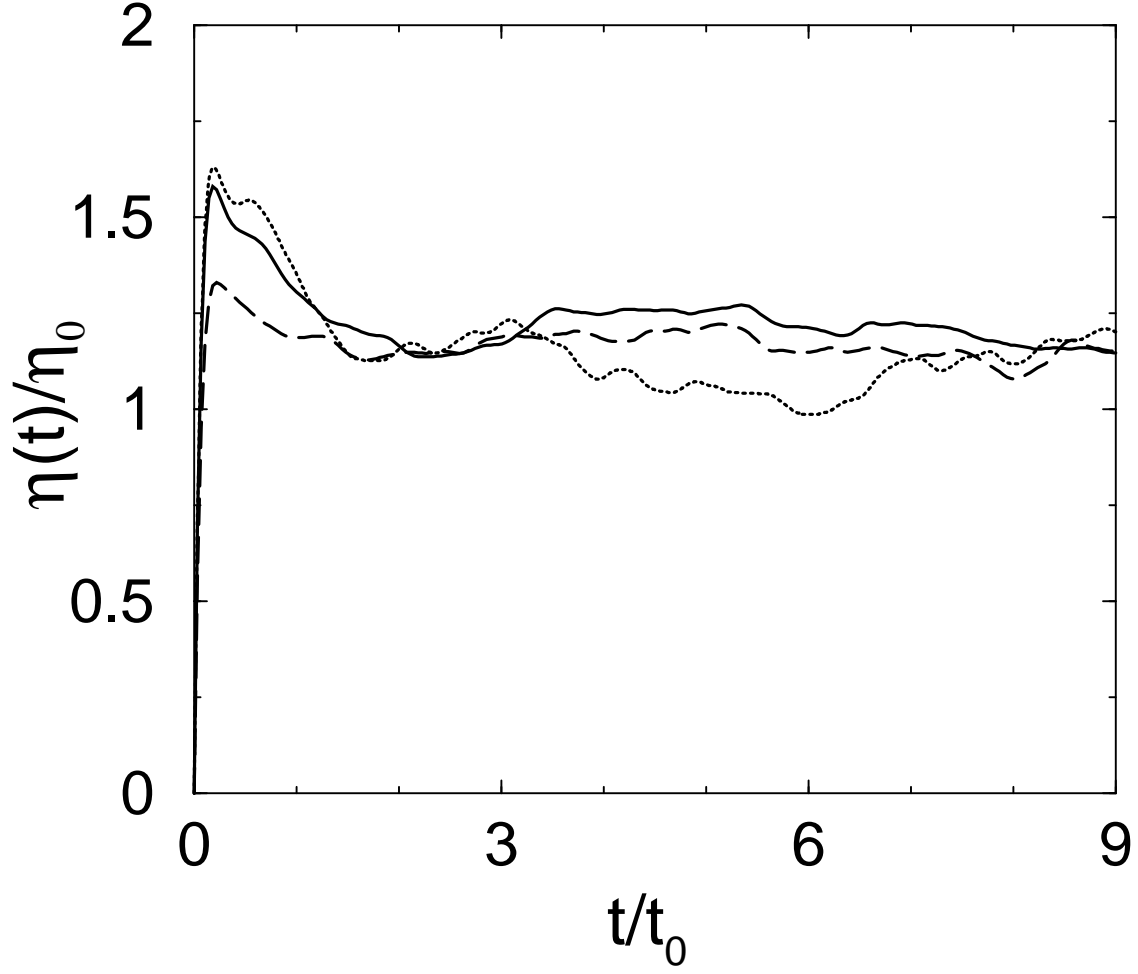


FIG. 6: Time dependent shear viscosity (normalized by the reference system value) for mixtures with  $\sigma_c/\sigma = 15$ ,  $m_c/m = 1000$  (solid line),  $\sigma_c/\sigma = 10$ ,  $m_c/m = 1000$  (dashed line), and  $\sigma_c/\sigma = 15$ ,  $m_c/m = 1$  (dotted line).

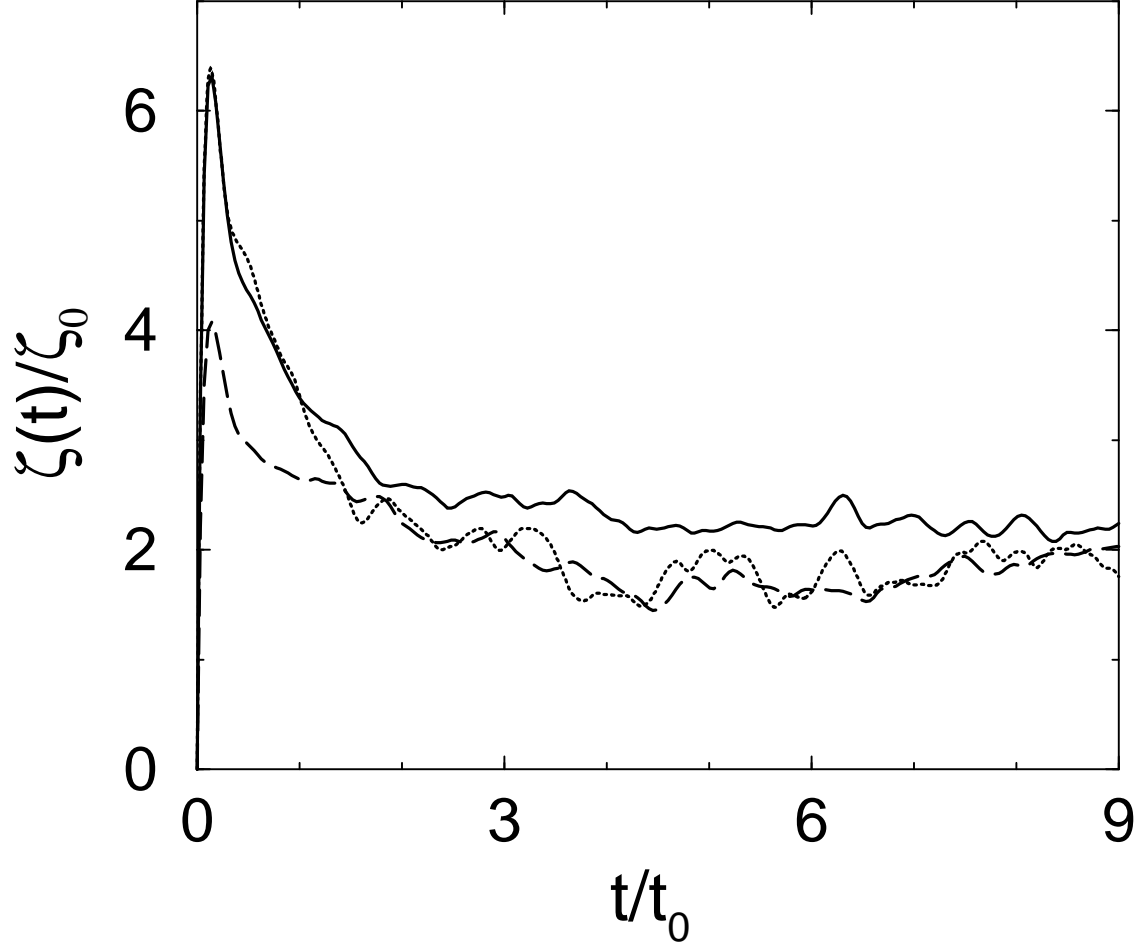


FIG. 7: Time dependent bulk viscosity (normalized by the reference system value) for mixtures with  $\sigma_c/\sigma = 15$ ,  $m_c/m = 1000$  (solid line),  $\sigma_c/\sigma = 10$ ,  $m_c/m = 1000$  (dashed line), and  $\sigma_c/\sigma = 15$ ,  $m_c/m = 1$  (dotted line).

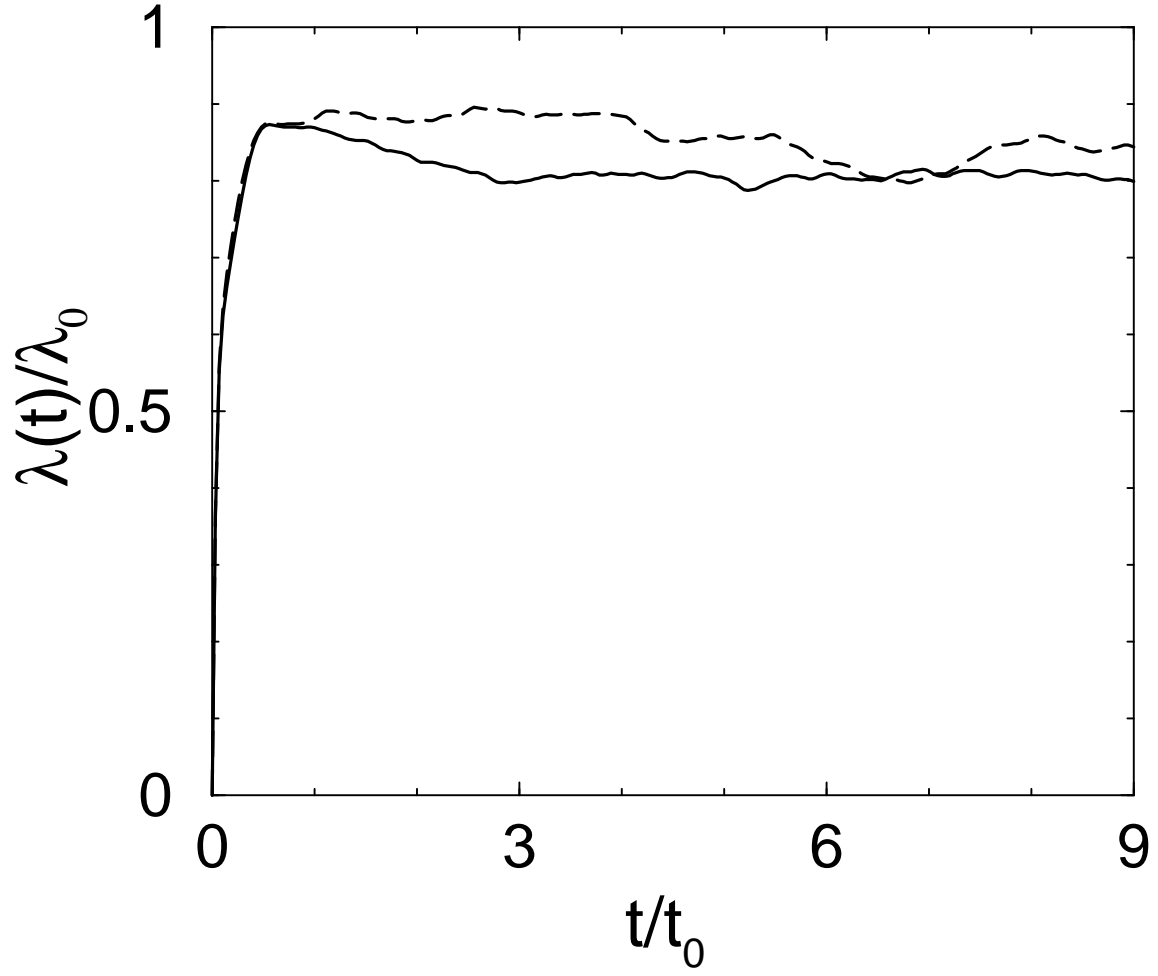


FIG. 8: Time dependent thermal conductivity (normalized by the reference system value) for mixtures with  $\sigma_c/\sigma = 15$ ,  $m_c/m = 1000$  (solid line),  $\sigma_c/\sigma = 10$ ,  $m_c/m = 1000$  (dashed line), and  $\sigma_c/\sigma = 15$ ,  $m_c/m = 1$  (dotted line).

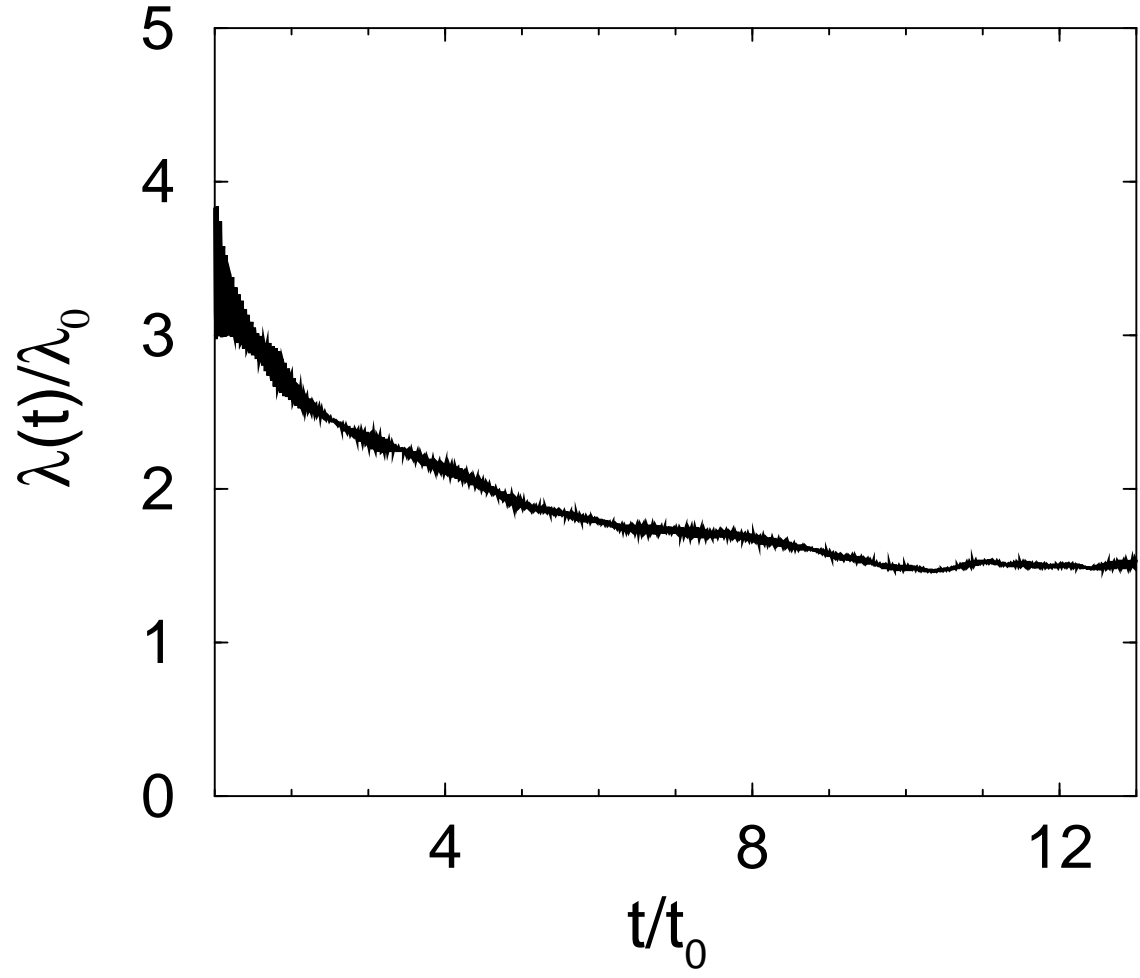


FIG. 9: Time dependent thermal conductivity (normalized by the reference fluid value) for the mixture with  $\sigma_c/\sigma = 15$  and  $m_c/m = 1$ .